

Back-Drivability Recovery of a Full Lower Extremity Assistive Robot

Byeonghun Na¹, Joonbum Bae², and Kyoungchul Kong^{1*}

¹Department of Mechanical Engineering, Sogang University, Seoul 121-742, Korea
(Tel : +82-2-701-9684; E-mail: {nbh87, kckong}@sogang.ac.kr)

²School of Mechanical and Advanced Materials Engineering, UNIST, Ulsan 689-798, Korea
(Tel : +82-52-217-2335; E-mail: jbbae@unist.ac.kr)

* Corresponding author

Abstract: Recently, walking assistance robots are receiving a great attention according to the increase of elderly population. Such systems are required to generate precise and large assistive torques to effectively assist human motions. Moreover, the assistive robots should be light and compact for the comfort and safety issues. In this paper we designed full lower extremity assistive robot with compact rotary series elastic actuators(cRSEAs) that are designed considering these factors. A worm gear is installed to amplify the motor torque in the limited space. Also, to generate assistive torque as desired, a torsional spring is used between the motor and the human joint. The device generates large assistive torques by utilizing worm gear, but the large friction introduced by the worm gear makes the controller design challenging. In this paper, a feedback control algorithm is proposed to compensate for such undesired disturbances. The proposed method is verified by experiments.

Keywords: Series elastic actuator, Impedance compensation, Walking assistance device.

1. INTRODUCTION

Mechatronic technologies play important roles in applications that improve quality of life. Some of the examples are active assistive devices, such as motorized wheel chairs or active prosthetics. They have improved the mobility of many people with disabilities, which allowed them to engage their everyday lives with much less difficulties. Recently, wearable robots for assisting physically impaired people or for augmenting human power have been developed which are based on mechatronic technologies[1]-[6].

As a representative, various assistive robots have been developed: Sankai developed Hybrid Assistive Limb(HAL) for augmenting power of healthy person [1][2], and Kazerooni introduced Berkeley Lower Extremity Exoskeleton(BLEEX) for military applications [3][4]. Ekso Bionics developed eLEGS and Rex bionics developed Robotic exoskeleton(Rex) for rehabilitation of the lower extremity [5][6].

Various control algorithm and actuators are used for such applications. The main role of the controller is to determine the direction and the magnitude of forces for interacting with a human (e.g., assistive forces or resistive forces for rehabilitation). In particular, controllers for human-robot interaction may assume that actuators are operated in an ideal force (or torque) mode control. The ideal force mode signifies that: 1) the actuator has (output shaft) zero impedance so that it is perfectly back-drivable; and 2) the force (torque) output is exactly proportional to the control input.

To achieve these requirements, electric motors equipped with gear reducers have been often used in the human assistive robots[1][6]. The gear reducers amplify the motor torque by reducing the rotor speed, but they increase the mechanical impedance of the system considerably. Also, the gear reducers increase stiffness of

the actuator, which is not desirable from the perspective of safety. Moreover, nonlinearities inherent in the gear reducers (e.g., backlash and friction) make the precise torque control difficulty.

To overcome such weak points of the geared motors while taking advantage of their superior controllability and high power-mass density, series elastic actuators have been introduced[7]-[13]. The series elastic actuators are actuator modules that consist of an electric motor and a spring. The spring arranged between the actuator and the human joint plays the role of an energy buffer as well as a torque sensor, which allows the precise control of generated torque. Because the spring is able to immediately store the impact forces exerted from the human joint, compliance can also be easily guaranteed depending on the control algorithm.

In our previous work, a rotary series elastic actuator(RSEA) and its robust control algorithm were presented [14]. The RSEA used a torsion spring and a geared DC motor. A disturbance observer was applied to precisely control the RSEA in the presence of nonlinearities inherent in the geared motor and model uncertainties caused by human-robot interactions. The proposed methods have shown good performance in practice (i.e., precise torque control, back-drivability, low impedance, etc) and have introduced to actual assistive devices.

In this paper, an improved design of the RSEA, a compact rotary series elastic actuator (cRSEA), and its control algorithm are proposed. The design parameters of the cRSEA are optimized to assist walking motions since the device is designed for lower extremity assistance. In the cRSEA, to amplify the torque generated by an electric motor, a worm gear is utilized as well as spur gears. However, the torque amplification ratio of the worm gear is sensitive to the friction coefficient, which introduces an uncertainty to the system model. Accordingly, the dy-

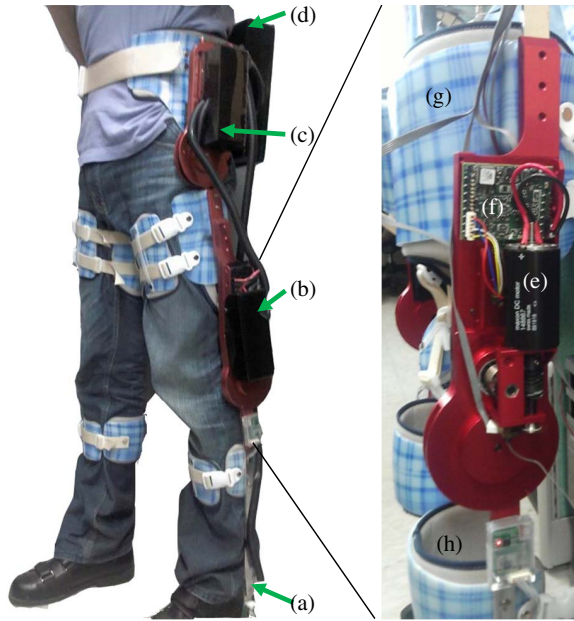


Fig. 1 Lower extremity assistive device and compact rotary series elastic actuator(cRSEA) module. (a) frame of orthosis, (b) the cRSEA module of knee joint, (c) the cRSEA module of hip joint, (d) a controller box with a Li-ion battery, (e) a DC motor, (f) a motor driver, (g) a thigh brace, and (h) a calf brace.

dynamic model of cRSEA is obtained regarding the friction between the worm wheel and the worm gear. Since the cRSEA is subjected to disturbances due to interactions with humans as well as large model variations, a robust control method is required.

In this paper, the design of controllers for a compact rotary series elastic actuator (cRSEA) is proposed. To guarantee the robust performance of the cRSEA, a high gain feedback controller is utilized.

2. HARDWARE CONFIGURATION

The lower extremity assistive device consists of 1) orthosis frame, 2) hip and knee joint cRSEA modules, 3) controller box with Li-ion battery, as shown in Fig. 1, and the compact rotary series elastic actuator (cRSEA) consists of a DC motor, a worm gear set, a spur gear set, a torsion spring, two high resolution encoders, a motor driver, as shown in Fig. 2. In this section, the mechanical design and the dynamic model of the cRSEA are introduced.

2.1 Kinematic Model

Fig. 2 shows the power transmission mechanism of the proposed cRSEA. The torque generated by the motor [(a) in the figure] is amplified by two sets of gears, the worm gear set [(b) and (c)] and the spur gear set [(e) and (f)]. The frame [(f) in the figure] is tied up the calf brace, while the main frame is connected to the thigh brace. Therefore, θ_H represents the knee joint angle. The small spur gear angle, θ_S , and the motor angle, θ_M , are measured by high resolution encoders.

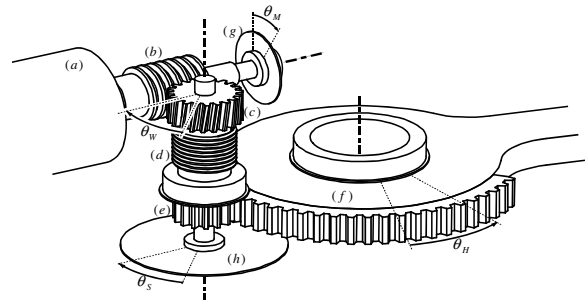


Fig. 2 Power transmission mechanism of cRSEA[15]. (a) Maxon RE40 DC motor, (b) a worm gear, (c) a worm wheel, (d) a torsional spring, (e) a small spur gear(fifteen teeth), (f) a knee frame with a large spur gear(ninety teeth), (g) an encoder on the motor side, and (h) an encoder on the human side.

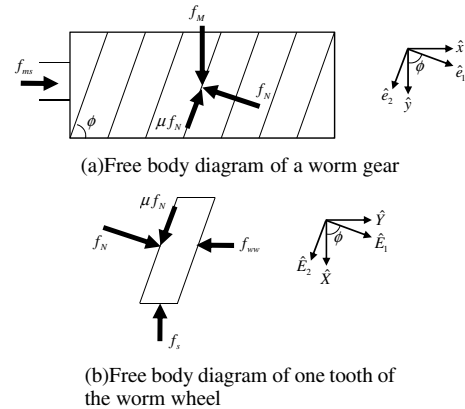


Fig. 3 Free body diagrams of the worm gear and worm wheel[15]. f_M represents the force generated by the motor, and f_{ms} , f_{ww} and f_s represent the reaction forces by the motor shaft, the worm wheel and the worm wheel shaft.

By a simple calculation, the knee joint angle, θ_H , can be obtained, i.e.

$$\theta_H = N_S^{-1} \theta_S \quad (1)$$

where N_S is the speed reduction ratio between the spur gear set [(e) and (f) in Fig. 2]. In the actual design, $N_S=6$.

Similarly, worm gear set provides the speed reduction ratio of N_W . When the worm gear rotates one revolution, one pitch of the worm wheel is rotated. Therefore, the worm gear acts as a single toothed gear, it means the gear ratio is the same as the number of teeth of the worm wheel. Since one revolution of the worm gear corresponds to one pitch of the worm wheel, the following kinematic condition is satisfied.

$$2\pi r_{wg} [\tan \phi]^{-1} = 2\pi r_{ww} N_W^{-1} \quad (2)$$

where r_{wg} and r_{ww} are the radii of the worm gear and the worm wheel, respectively. ϕ is the distortion angle of the worm gear shown in Fig. 3. Note that (2) can be simplified to $N_W = [r_{ww}/r_{wg}] \tan \phi$.

2.2 Dynamic Model

Fig. 3 shows the free body diagrams of the worm gear and worm wheel installed in the cRSEA [(b) and (c) in Fig. 2]. The force vectors in Fig. 3 are acting on the point that the worm gear contacts the worm wheel. Note that the contact point moves only in the direction of \hat{y} or \hat{Y} due to mechanical constraints.

From the force balance equations, dynamic equation can be derived, i.e.

$$N_S k(\theta_W - \theta_S) = N_S A(\phi, \mu) \left[\tau_M - \left(\frac{I_{WW}}{N_W A(\phi, \mu)} + I_M \right) \ddot{\theta}_M \right] - \tau_H \quad (3)$$

where

$$A(\phi, \mu) = \frac{r_{WW}(\sin \phi + \mu \cos \phi)}{r_{WG}(\cos \phi + \mu \sin \phi)} \quad (4)$$

$A(\phi, \mu)$ in (4) is a torque amplification ratio of the worm gear and the worm wheel. In the actual cRSEA, the distortion angle of the worm gear, ϕ , is fixed, but the friction coefficient, μ , may vary depending on the lubricant or temperature conditions. The variation in the torque amplification ratio introduces model uncertainties to the system.

The dynamic model in (3) shows that the cRSEA is a multi-input and multi-output system, where the inputs are the motor torque [τ_M , control input] and the human joint torque [τ_H , disturbance input], and the outputs are the motor angle [θ_M] and the angle of the spur gear [θ_S]. The generated torque, τ_O , can be calculated by Hooke's law from the measured angles.

3. CONTROLLER DESIGN OF COMPACT ROTARY SERIES ELASTIC ACTUATOR

The performance objectives of the cRSEA are 1) to precisely generate the desired torque in spite of model uncertainties and external disturbances, 2) to minimize the mechanical impedance for back-drivability, and 3) to minimize the influence of human motions in the generated torques. In (3), note that the torque output, $\tau_O = N_S k(\theta_W - \theta_S)$, is influenced by the angular acceleration of the motor shaft, $\ddot{\theta}_M$, and the torques exerted from the human side, τ_H . The variation in $A(\phi, \mu)$ also introduces an uncertainty to the system. In this section, a robust control algorithm is designed to meet the performance objectives considering these factors.

Suppose the following control law:

$$\tau_M = K_P(r - \tau_O) + K_D(\dot{r} - \dot{\tau}_O) + K_I \int (r - \tau_O) dt \quad (5)$$

where r is the reference input, and τ_O is the torque output generated by the spring [i.e., $\tau_O = N_S k(\theta_W - \theta_S)$]. Note that τ_O can be directly calculated from $\theta_W = N_W^{-1} \theta_M$ and θ_S , which are measured by encoders. The parameters K_P , K_D , and K_I are controller gains to have the torque output follow the reference input. Fig. 4 shows the block diagram of the proposed control law.

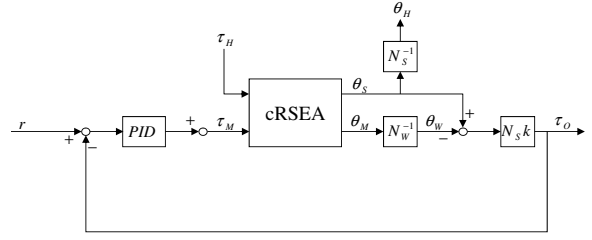


Fig. 4 Block diagram of the proposed control law[15]. N_W and N_S represent the speed reduction ratio of the worm gear set and the spur gear set, PID represent the PID controller in (5).

By applying the Laplace transformation to the remaining closed loop dynamics, a transfer function is

$$\tau_O = G_{R \rightarrow O}(s)r - G_{H \rightarrow O}(s)\tau_H \quad (6)$$

where

$$G_{R \rightarrow O}(s) = \frac{K_D s^2 + (K_P + N_S^{-1} N_W^{-1})s + K_I}{K_D s^2 + (K_P + N_S^{-1} A^{-1})s + K_I} \quad (7)$$

$$G_{H \rightarrow O}(s) = \frac{N_S^{-1} A^{-1} s}{K_D s^2 + (K_P + N_S^{-1} A^{-1})s + K_I} \quad (8)$$

where $G_{R \rightarrow O}(s)$ is the transfer functions to the torque output from the reference input and $G_{H \rightarrow O}(s)$ is the transfer functions to the torque output from the human joint torque.

The controller gains K_P , K_D , and K_I can be designed considering the desired closed loop poles. In the controller design, the torque amplification ratio, $A(\phi, \mu)$, is regarded as its nominal value, N_W . Note that $G_{R \rightarrow O}(s)$ and $G_{H \rightarrow O}(s)$ respectively become close to 1 and 0, as the magnitude of controller gains increases.

4. PERFORMANCE ANALYSIS BY EXPERIMENTS

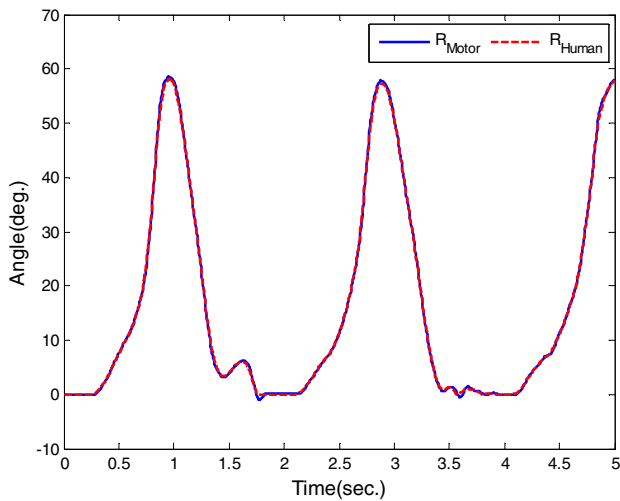
Once an cRSEA is stabilized by applying the overall control system shown in Fig. 4, it is desired to evaluate the following performance objectives by experiments:

1. capability of rejecting the undesired disturbances including the rotor inertia and any disturbances, i.e., the controlled cRSEA exhibits low impedance;
2. capability of generating the desired torque precisely;

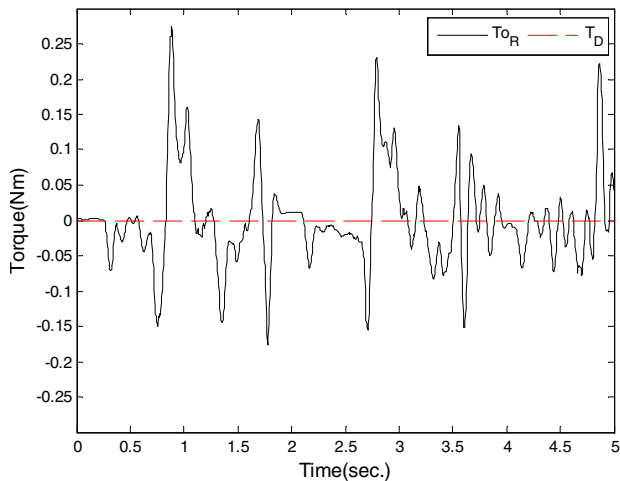
To verify the performance of the control system, cRSEAs were installed at an active orthosis system, as shown in Fig. 1. Four cRSEAs were attached to each hip and knee joint, and controlled by the proposed control algorithm.

Setting the desired torque to zero, a subject wearing the active orthosis was walking on a treadmill. It is desired that the subject does not feel any resistance from the actuators, i.e., the actuator followed the human joint motion to keep zero spring deflection.

Fig. 5 shows the right knee motion and the resistive torque generated by the actuator. The motor followed the human joint motion with a time delay of a few samples,



(a) Motor angle θ_M and the knee angle θ_H



(b) Desired and resistive torque

Fig. 5 Experimental data on right knee joint during walking: the desired assistive torque was zero.



Fig. 6 Outdoor experiment with full lower extremity assistive robot.

as shown in Fig. 5(a). The maximum tracking error was 1.36 deg . Fig. 5(b) shows the resistive torque generated by the actuator. The resistive torque was large at high angular velocities (e.g., about 1.0s). The generated resistive torque was $5.05 \times 10^{-4} \text{ Nm}$ in root-mean-square and $4.50 \times 10^{-1} \text{ Nm}$ in peak-to-peak. The magnitude of the resistive torque was small so that the subject did not feel any resistance.

The device, full lower extremity robot, is designed for outdoor application. Fig. 6 shows outdoor environment experimental situation. In case of coming down the stairs, the subject did not feel any discomfort with the full lower extremity assistive robot. In addition, when walking on a track, the subject could move smoothly.

5. CONCLUSION

In human-robot interaction applications, actuators should have zero impedance for precise force control. In spite of numerous efforts, the actuator design is still one of the most critical problems in this field. In this paper, full lower extremity assistive robot with cRSEA module was designed, and its control method was proposed for improved human-robot interaction.

The proposed actuation module, cRSEA, uses a torsion spring in the chain of spur gears and worm gears, which allows the precise control of the generated assistive torque. The performance of the proposed robot and control algorithm (e.g., to minimize the impedance and to generate the desired torque precisely) was verified by experiments.

ACKNOWLEDGEMENT

This research was supported by Basic Science Research Program through the National Research Foundation of Korea (NRF) funded by the Ministry of Education, Science and Technology (2012R1A1A1008271).

REFERENCES

- [1] T. Hayashi, H. Kawamoto, and Y. Sankai, "Control method of robot suit HAL working as operators muscle using biological and dynamical information," in *Proc. IEEE/RSJ Int. Conf. Intell. Robots Syst. (IROS 2005)*, pp. 3063-3068.
- [2] Cyberdyne Company, HAL-5 [Online]. Available: <http://www.cyberdyne.jp>
- [3] H. Kazerooni, J. Racine, L. Huang, and R. Steger, "On the control of the Berkeley Lower Extremity Exoskeleton (BLEEX)," in *Proc. IEEE Int. Conf. Robotics Autom. (ICRA 2005)*, pp. 4353-4360.
- [4] A. Zoss, H. Kazerooni, and A. Chu, "Biomechanical design of the Berkeley Lower Extremity Exoskeleton (BLEEX)," *IEEE/ASME Trans. Mechatronics*, vol. 11, no. 2, pp. 128-138, Apr. 2006.
- [5] Eksobionics Company, eLEGS [Online]. Available: <http://www.eksobionics.com/>
- [6] Rexbionics Company, Rex [Online]. Available: <http://www.rexbionics.com>

- [7] D. Paluska and H. Herr, "Series elasticity and actuator power output," in *Proc. IEEE Int. Conf. Robotics Autom. (ICRA 2006)*, pp. 1830-1833.
- [8] K. Kong and M. Tomizuka, "Flexible joint actuator for patients rehabilitation device," in *Proc. IEEE Int. Symp. Robot Human Interactive Commun. (ROMAN 2007)*, pp. 1179-1184.
- [9] J. Pratt, B. Krupp, and C. Morse, "Series elastic actuators for high fidelity force control," *Int. J. Ind. Robot*, vol. 29, no. 3, pp. 234-241, 2002.
- [10] K. H. Low, "Initial experiments of a leg mechanism with a flexible geared joint and footpad," *Adv. Robot.*, vol. 19, no. 4, pp. 373-399, 2005.
- [11] G. A. Pratt and M. Williamson, "Series elastic actuators," in *Proc. IEEE/RSJ Int. Conf. Intell. Robot. Syst. (IROS 1995)*, pp. 399-406.
- [12] D.W. Robinson, J. E. Pratt, D. J. Paluska, and G. A. Pratt, "Series elastic actuator development for a biomimetic walking robot," in *Proc. IEEE/RSJ Int. Conf. Intell. Robot. Syst. (IROS 1995)*, pp. 561-568.
- [13] M. M. Williamson, "Series elastic actuators," M. S. thesis, Massachusetts Inst. Technol., Cambridge, Jun. 1995.
- [14] K. Kong, J. Bae, and M. Tomizuka, "Control of rotary series elastic actuator for ideal force-mode actuation in human-robot interaction applications," *IEEE/ASME Trans. Mechatronics*, vol. 14, pp. 105-118, 2009.
- [15] K. Kong, J. Bae, and M. Tomizuka, "A Compact Rotary Series Elastic Actuator for Human Assistive Systems," *IEEE/ASME Trans. Mechatronics*, vol. 17, no. 2, pp. 288-297, Apr. 2012.